Elastic e-d Scattering Data and the Deuteron Wave Function

R. Schiavilla

Jefferson Lab, Newport News, Virginia 23606

and

Department of Physics, Old Dominion University, Norfolk, Virginia 23529

V.R. Pandharipande

Department of Physics, University of Illinois at Urbana-Champaign, Urbana, IL 61801

(January 13, 2002)

Abstract

What range of momentum components in the deuteron wave function are available ed elastic scattering data sensitive to ? This question is addressed within the context of a model calculation of the deuteron form factors, based on realistic interactions and currents. It is shown that the data on the $A(q)$, $B(q)$, and $T_{20}(q)$ observables at $q \leq 6$ fm^{-1} essentially probe momentum components up to $\simeq 4\,m_\pi$.

21.30.+y, 21.45.+v, 27.10.+h

Typeset using REVTEX

I. INTRODUCTION, RESULTS, AND CONCLUSIONS

The present work addresses the following issue: what range of momentum components in the deuteron wave function are probed by presently available *e-d* elastic scattering data ? The question is answered within the context of a model calculation [1], based on realistic interactions and currents, that predicts quite well the observed deuteron $A(q)$ and $B(q)$ structure functions and $T_{20}(q)$ tensor polarization up to momentum transfers $q \simeq 6$ fm^{-1}. To this end, the deuteron S- and D-wave components obtained in the full theory [1] and denoted as $u_L(p)$, L=0, 2, are truncated, in momentum space, as

$$\overline{u}_L(p;n) = \frac{c_n}{\left[1+\exp(p-p_n)/a\right]^{1/2}}\, u_L(p) \ , \tag{1.1}$$

where the cutoff momentum p_n=$n\, m_\pi$ (m_π is the pion mass and n is an integer) and a=0.1 m_π. The constants c_n are fixed through the normalization condition, Eq. (2.6) below. The wave functions $\overline{u}_L(p;n)$ corresponding to n=1, 2 and 4 along with the reference $u_L(p)$ are shown in Fig. 1. The $A(q)$, $B(q)$, and $T_{20}(q)$ observables are calculated using these truncated wave functions by including one-body only and both one- and two-body currents. The results are displayed in Figs. 2-4.

Aspects of the present theory [1] pertaining to the input potential, the boost corrections in the wave functions, the one and two-body charge and current operators, are succinctly summarized in Secs. II–IV. Here it suffices to note that the results shown in Figs. 2–4 are obtained within a scheme in which these various facets are consistently treated to order $(v/c)^2$. Thus the present approach improves and extends that adopted in Refs. [2] and [3], in which relativistic corrections of order $(v/c)^2$ were selectively retained. For example, the $(v/c)^2$ contributions associated with the π-exchange charge operator were included, while those originating from the one-pion-exchange potential and from boosting the wave function were ignored. The consistent $(v/c)^2$ scheme employed here, however, does not alter quantitatively the predictions obtained in Refs. [2,3], except for the $B(q)$ structure function as discussed in Sec. V. A detailed analysis of the differences between the two approaches is beyond the scope of this work; it will be presented in Ref. [1].

We assume that the three-momentum transfer $\mathbf{q}$ in e-d elastic scattering is in the z-direction. In the Breit frame the deuteron has initial and final momenta $-q/2$ and $+q/2$ in this direction, respectively. In the presence of only single-nucleon currents, the deuteron wave function has to have components with relative momenta p=$\mid \mathbf{p}_1 - \mathbf{p}_2 \mid /2$ larger than $q/4$ in order to produce elastic scattering at momentum transfer q. In a limiting case, for example, the nucleons have momenta of $-q/2$ and 0 in the initial state and $+q/2$ and 0 in the final, all along the z-axis. Thus elastic scattering via one-body currents probes momentum distributions $u_L(p)$ at $p > q/4$. This argument, however, does not establish the maximum value of p which the observed form factors with $q \leq 6$ fm^{-1} are sensitive to. In addition, there is no kinematical limit on initial and final relative momenta for scattering via pair currents. Therefore, we use a realistic model of the deuteron to estimate the maximum value of p probed by the available data.

There is growing interest in chiral effective field theories of nuclear forces and currents [4,5]. In such theories the effective Lagrangian is obtained after integrating out states with momenta greater than a specified cutoff. We hope that the present results provide an estimate of the deuteron structure obtained in theories with cutoff momentum p_n=$n\,m_\pi$.

The deuteron wave function is dominated by the one-pion exchange potential $v_\pi(\mathbf{k})$, where $\mathbf{k}$=$\mathbf{p}' - \mathbf{p}$ is the momentum transferred by the exchanged pion. The dependence of $v_\pi(\mathbf{k})$ (see Eq. (2.2) below) on the magnitude k is primarily given by the πNN form factor $f_\pi(k)$ for $k > m_\pi$. In this limit the leading non-relativistic term of $v_\pi(\mathbf{k})$ becomes:

$$\begin{aligned} v_\pi(\mathbf{k}) &= -\frac{f_{\pi NN}^2}{m_\pi^2}\frac{f_\pi^2(k)}{m_\pi^2+k^2}\,\boldsymbol{\sigma}_1\cdot\mathbf{k}\,\boldsymbol{\sigma}_2\cdot\mathbf{k}\,\boldsymbol{\tau}_1\cdot\boldsymbol{\tau}_2 \\ &\simeq -\frac{f_{\pi NN}^2}{m_\pi^2}\,f_\pi^2(k)\,\boldsymbol{\sigma}_1\cdot\hat{\mathbf{k}}\,\boldsymbol{\sigma}_2\cdot\hat{\mathbf{k}}\,\boldsymbol{\tau}_1\cdot\boldsymbol{\tau}_2\ , \end{aligned} \tag{1.2}$$

where $\hat{\mathbf{k}}$ is a unit vector. Thus the deuteron wave function at momentum p is expected to be sensitive to $f_\pi(k)$ up to $k \simeq p$.

The results shown in Figs. 2–4 indicate that the available data on deuteron form factors at $q \leq 6$ fm^{-1} confirm the present wave functions up to $p \simeq 4\,m_\pi$. After including pair-current contributions, the reference wave function and that truncated at p=$4\,m_\pi$ do not

give significantly different form factors in this q-range. The reference and truncated wave functions, respectively, over- and under-predict the observed $A(q)$ at $q \geq 6$ fm^{-1}; both under-predict $B(q < 7$ fm$^{-1})$, and fail to reproduce the data point for T_{20} at $q \simeq 6.8$ fm^{-1}. The available data on $A(q)$ at larger values of q can be used to test the deuteron wave function at $p > 4\,m_\pi$; however, improved theoretical understanding and more accurate data on $B(q > 6$ fm$^{-1})$, and new data on $T_{20}(q > 6$ fm$^{-1})$ are needed.

II. DEUTERON WAVE FUNCTION

The deuteron rest-frame wave function is obtained by solving the momentum-space Schrödinger equation with the relativistic Hamiltonian [6,7]

$$H^\mu = 2\sqrt{p^2 + m^2} + v^\mu \ , \tag{2.1}$$

where v^μ consists of a short-range part v^μ_R parameterized as in the Argonne v_{18} potential [3], and of a relativistic one-pion-exchange potential (OPEP) given by

$$\begin{aligned} v^\mu_\pi(\mathbf{p}'_1, \mathbf{p}_1) = & -\frac{f^2_{\pi NN}}{m^2_\pi}\frac{f^2_\pi(k)}{m^2_\pi + k^2}\frac{m}{E'}\frac{m}{E}\Bigg[\boldsymbol{\sigma}_1 \cdot \mathbf{k}\,\boldsymbol{\sigma}_2 \cdot \mathbf{k} \\ & + \mu \times (E' - E)\left(\frac{\boldsymbol{\sigma}_1 \cdot \mathbf{p}'_1\,\boldsymbol{\sigma}_2 \cdot \mathbf{p}'_1}{E' + m} - \frac{\boldsymbol{\sigma}_1 \cdot \mathbf{p}_1\,\boldsymbol{\sigma}_2 \cdot \mathbf{p}_1}{E + m}\right)\Bigg]\boldsymbol{\tau}_1 \cdot \boldsymbol{\tau}_2 \ . \end{aligned} \tag{2.2}$$

Here m is the nucleon mass, $f_{\pi NN}$ is the pion-nucleon coupling constant ($f^2_{\pi NN}/4\pi$=0.075), $\mathbf{p}_1$ and $\mathbf{p}'_1$ are the initial and final momenta of particle 1 in the center-of-mass frame, $\mathbf{k}$=$\mathbf{p}'_1 - \mathbf{p}_1$ is the momentum transfer, E=$\sqrt{p_1^2 + m^2}$, and E'=$\sqrt{p_1'^2 + m^2}$. The monopole form factor:

$$f_\pi(k) = \frac{\Lambda^2_\pi - m^2_\pi}{\Lambda^2_\pi + k^2} \ , \tag{2.3}$$

with Λ_π=1.2 GeV/c is used in this work.

The μ-dependent term characterizes possible off-energy-shell extensions of OPEP, and leads to strong non-localities in configuration space. In particular, the value μ=-1 (μ=1) is predicted by pseudoscalar (pseudovector) coupling of pions to nucleons, while μ=0 corresponds to the so-called "minimal non-locality" choice [8]. It has been known for over two

decades [8], and recently re-emphasized by Forest [7] that these various off-shell extensions of OPEP are related to each other by a unitary transformation, in the sense that

$$\mathrm{e}^{-\mathrm{i}\mu U} H^{\mu=0} \mathrm{e}^{\mathrm{i}\mu U} \simeq H^{\mu=0} + \mathrm{i}\mu \Big[H^{\mu=0}\,,\, U \Big] \simeq H^{\mu} \ , \tag{2.4}$$

if terms of 2π-range (and shorter-range) are neglected. The hermitian operator U is given explicitly in Ref. [7]. This unitary equivalence implies that predictions for electromagnetic observables, such as the form factors under consideration here, are independent of the particular off-shell extension adopted for OPEP, provided that the electromagnetic current operator, specifically its two-body components associated with pion exchange, are constructed consistently with this off-shell parameter. This point will be further elaborated below. At this stage, however, it is important to recall that Forest has constructed relativistic Hamiltonians H^{μ} with $\mu{=}\pm 1, 0$, each designed to be phase-equivalent to the non-relativistic H, based on the Argonne v_{18} potential.

Given this premise, the $\mu{=}0$ prescription is adopted for OPEP from now on, and the superscript is dropped from $H^{\mu=0}$, for ease of presentation. The resulting momentum-space wave function in the rest frame of the deuteron is denoted with $\psi_M(\mathbf{p};0)$ (here, the argument 0 indicates the rest frame in which the deuteron has velocity $\mathbf{v}{=}0$), and is written as

$$\psi_M(\mathbf{p};0) = \Big[u_0(p) \mathcal{Y}^M_{011}(\hat{\mathbf{p}}) + u_2(p) \mathcal{Y}^M_{211}(\hat{\mathbf{p}}) \Big] \eta^0_0 \ , \tag{2.5}$$

where $\mathbf{p}$ is the relative momentum, M is the angular-momentum projection along the z-axis, η^0_0 is the pair isospin $T{=}0$ state, and $\mathcal{Y}^M_{LSJ}(\hat{\mathbf{p}})$ are standard spin-angle functions. The normalization is given by:

$$\int_0^{\infty} \frac{\mathrm{d}p\, p^2}{(2\pi)^3} [u_0^2(p) + u_2^2(p)] = 1 \ . \tag{2.6}$$

The internal wave function in a frame moving with velocity $\mathbf{v}$ with respect to the rest frame can be written to order $(v/c)^2$ as [8]

$$\begin{aligned} \psi_M(\mathbf{p};\mathbf{v}) &\simeq \left(1 - \frac{v^2}{4}\right) \left[1 - \frac{1}{2}(\mathbf{v}\cdot\mathbf{p})(\mathbf{v}\cdot\nabla_p) - \frac{\mathrm{i}}{4m}\mathbf{v}\cdot(\boldsymbol{\sigma}_1 - \boldsymbol{\sigma}_2)\times\mathbf{p} \right] \psi_M(\mathbf{p};0) \\ &\simeq \frac{1}{\sqrt{\gamma}} \left[1 - \frac{\mathrm{i}}{4m}\mathbf{v}\cdot(\boldsymbol{\sigma}_1 - \boldsymbol{\sigma}_2)\times\mathbf{p} \right] \psi_M(\mathbf{p}_{\parallel}/\gamma, \mathbf{p}_{\perp};0) \ , \end{aligned} \tag{2.7}$$

where $\gamma = 1/\sqrt{1-v^2}$, and $\mathbf{p}_\parallel$ and $\mathbf{p}_\perp$ denote the components of the momentum $\mathbf{p}$ parallel and perpendicular to $\mathbf{v}$, respectively. Only the kinematical boost corrections, associated with the Lorentz contraction (term $\propto \mathbf{v}\cdot\mathbf{p}\,\mathbf{v}\cdot\nabla_p$) and Thomas precession of the spins (term $\propto \mathbf{v}\cdot(\boldsymbol{\sigma}_1-\boldsymbol{\sigma}_2)\times\mathbf{p}$) are retained in Eq. (2.7). There are in principle additional, interaction-dependent boost corrections. Those originating from the dominant one-pion-exchange component of the interaction have been constructed explicitly in Ref. [8] to order $(v/c)^2$. At this order, however, their contribution to the form factors in Eqs. (4.5)–(4.7) vanishes, since it involves matrix elements of an odd operator under spin exchange between S=1 states. Indeed, this same selection rule also holds for the Thomas precession term. Therefore the interaction-dependent boost corrections do not contribute to elastic scattering up to order $(v/c)^2$, and are neglected in the following.

It should also be noted that terms of order higher than $(v/c)^2$ due to Lorentz contraction have in fact been included in the second line of Eq. (2.7). The factor $1/\sqrt{\gamma}$ ensures that the wave function in the moving frame is normalized to one, ignoring corrections of order $(v/c)^4$ from the Thomas precession term.

It is interesting to study the relation between the Breit-frame matrix element $\overline{\rho}(\mathbf{q};B)$ of the point-nucleon density operator, and the rest frame $\overline{\rho}(\mathbf{q};0)$. One finds, again ignoring Thomas precession contributions:

$$\begin{aligned}\overline{\rho}_M(\mathbf{q};B) &= \int \frac{\mathrm{d}\mathbf{p}}{(2\pi)^3}\psi^\dagger_M(\mathbf{p}+\mathbf{q}/4;\mathbf{v}_B)\;\psi_M(\mathbf{p}-\mathbf{q}/4;-\mathbf{v}_B)\\ &= \frac{1}{\gamma_B}\int \frac{\mathrm{d}\mathbf{p}}{(2\pi)^3}\psi^\dagger_M\left(\frac{\mathbf{p}_\parallel+\mathbf{q}/4}{\gamma_B},\mathbf{p}_\perp;0\right)\;\psi_M\left(\frac{\mathbf{p}_\parallel-\mathbf{q}/4}{\gamma_B},\mathbf{p}_\perp;0\right)\\ &= \overline{\rho}_M(\mathbf{q}/\gamma_B;0)\;,\end{aligned} \tag{2.8}$$

after rescaling of the integration variables, $(\mathbf{p}_\parallel/\gamma_B,\mathbf{p}_\perp)\rightarrow(\mathbf{p}_\parallel,\mathbf{p}_\perp)$, in the last integral. Here γ_B is the Lorentz factor corresponding to $\mathbf{v}_B = (q/2)\hat{\mathbf{z}}/\sqrt{q^2/4+m_d^2}$ in the Breit frame. This result is consistent with the naive expectation that the density in configuration space is "squeezed" in the direction of motion by the Lorentz factor γ_B or, equivalently, that its Fourier transform is "pushed out" by γ_B. For q=6 fm^{-1}, $v_B \simeq 0.3$ and $\gamma_B \simeq 1.05$, corresponding to a 5 % Lorentz contraction.

III. NUCLEAR ELECTROMAGNETIC CURRENT

The electromagnetic charge and current operators include one- and two-body terms. Only the isoscalar parts need to be considered, since the deuteron has T=0. The one-body term is taken as

$$j^\sigma_{1-\rm body}(\mathbf{q}) = (\rho_{1-\rm body}(\mathbf{q}), \mathbf{j}_{1-\rm body}(\mathbf{q})) = \sum_{i=1,2} \frac{1}{2}\overline{u}'_i \left[F_1^S(q)\gamma^\sigma + \mathrm{i}\frac{F_2^S(q)}{2m}\sigma^{\sigma\tau}q_\tau \right] u_i \ , \qquad (3.1)$$

where q^σ=$(0, q\hat{\mathbf{z}})$ in the Breit frame, u_i and u'_i are the initial and final spinors of nucleon i, respectively, with $\overline{u}_i \equiv u_i^\dagger\gamma^0$, and F_1^S and F_2^S denote the isoscalar combinations of the nucleon's Dirac and Pauli form factors, normalized as $F_1^S(0)$=1 and $F_2^S(0)$=−0.12 (in units of n.m.). The Höhler parameterization [9] of F_1 and F_2 is used in this work. The spinor u, or rather its transpose, is given by

$$u^T = \left(\frac{E+m}{2E}\right)^{1/2} \left(\chi_s \, , \, \frac{\boldsymbol{\sigma}\cdot\mathbf{p}}{E+m}\chi_s\right) \ , \qquad (3.2)$$

where $\mathbf{p}$ and E=$\sqrt{p^2+m^2}$ are the nucleon's momentum and energy, and χ_s is its (two-component) spin state. Note that $u^\dagger u$=1. In earlier published work on the form factors of the deuteron [2,3] and A=3–6 nuclei, most recently [10,11], boost contributions were neglected, and only terms up to order $(v/c)^2$ were included in the non-relativistic expansion of $j^\sigma_{1-\rm body}$, namely the well known Darwin-Foldy and spin-orbit corrections to $\rho(\mathbf{q})$. In the calculations reported here, however, the full Lorentz structure of $j^\sigma_{1-\rm body}$ is retained.

The two-body terms included in $j^\sigma_{2-\rm body}$ are those associated with π- and ρ-meson exchanges and the $\rho\pi\gamma$ transition mechanism. The π and ρ spatial current operators to leading order in v/c are isovector, and therefore their contributions vanish in e-d elastic scattering. The π-exchange charge operator is obtained, consistently with the off-shell parameter μ adopted for OPEP, as [8]

$$\rho^\mu_\pi(\mathbf{q}) = \frac{(3-\mu)}{8m}\frac{f^2_{\pi NN}}{m^2_\pi}F_1^S(q)\frac{f_\pi(k_2)}{k_2^2+m_\pi^2}\boldsymbol{\sigma}_1\cdot\mathbf{q}\ \boldsymbol{\sigma}_2\cdot\mathbf{k}_2\,\boldsymbol{\tau}_1\cdot\boldsymbol{\tau}_2 + 1 \rightleftharpoons 2 \ , \qquad (3.3)$$

where $\mathbf{k}_i$=$\mathbf{p}'_i - \mathbf{p}_i$, $f_\pi(k)$ is the πNN form factor defined in Sec. II, and $F_1^S(q)$ denotes the Höhler parameterization [9] for the nucleon's isoscalar Dirac form factor. It is easy to show, to order $(v/c)^2$, that

$$e^{-i\mu U}\left(\rho_{1-\mathrm{body}}+\rho_\pi^{\mu=0}\right)e^{i\mu U}\simeq\rho_{1-\mathrm{body}}+\rho_\pi^{\mu=0}+i\mu\Big[\rho_{1-\mathrm{body}}\,,\,U\Big]\simeq\rho_{1-\mathrm{body}}+\rho_\pi^{\mu}\ , \qquad (3.4)$$

where $\exp(-i\mu U)$ is the unitary transformation of Sec. II. Again, we emphasize that the choice μ=0 is made for ρ_π^μ (as for OPEP in Sec. II) in the present work.

At this point it is important to recall that the π-exchange charge operator corresponding to μ=−1 was included in all our previous studies of light nuclei form factors (for a review, see Ref. [12]), based on non-relativistic Hamiltonians, in which the OPEP part of v was taken to be its leading local form, i.e. E'=E and $E/m\rightarrow 1$ in Eq. (2.2). While these calculations are not strictly consistent, since relativistic corrections are selectively retained in $\rho(\mathbf{q})$ but ignored in the potentials and wave functions, they nevertheless give fairly accurate results since the corrections to the wave function are rather small [6].

Vector-meson (ρ and ω) two-body charge operators have been found to give contributions, in calculations of light nuclei form factors [12], that are typically an order of magnitude smaller than those associated with the ρ_π operator. In the present study, only the ρ-exchange charge operator is considered:

$$\rho_\rho(\mathbf{q})=\frac{g_{\rho NN}^2(1+\kappa_{\rho NN})^2}{8m^3}F_1^S(q)\frac{f_\rho(k_2)}{k_2^2+m_\rho^2}\,(\boldsymbol{\sigma}_1\times\mathbf{q})\cdot(\boldsymbol{\sigma}_2\times\mathbf{k}_2)\,\boldsymbol{\tau}_1\cdot\boldsymbol{\tau}_2+1\rightleftharpoons 2\ , \qquad (3.5)$$

where m_ρ, $g_{\rho NN}$ and $\kappa_{\rho NN}$ are the ρ-meson mass, vector and tensor coupling constants, respectively. Here the values $g_{\rho NN}^2/(4\pi)$=0.84, and $\kappa_{\rho NN}$=6.1 are used from the Bonn 2000 potential [13], while the ρNN monopole form factor $f_\rho(k)$ has Λ_ρ=1.2 GeV/c.

Finally, the $\rho\pi\gamma$ current is obtained from the associated Feynman amplitude as

$$\begin{aligned} j_{\rho\pi\gamma}^\mu(\mathbf{q})=&\,ig_{\rho\pi\gamma}\frac{g_{\rho NN}}{m_\rho}\frac{f_{\pi NN}}{m_\pi}G_{\rho\pi\gamma}(q)\,\frac{f_\rho(k_1)}{k_1^2+m_\rho^2}\,\frac{f_\pi(k_2)}{k_2^2+m_\pi^2}\,\epsilon^{\mu\nu\sigma\tau}k_{1,\sigma}q_\tau \\ &\times\left[\overline{u}_1'\left(\gamma_\nu+i\frac{\kappa_{\rho NN}}{2m}\sigma_{\nu\alpha}k_1^\alpha\right)u_1\right]\left(\overline{u}_2'\,\gamma_\beta k_2^\beta\,\gamma_5 u_2\right)\boldsymbol{\tau}_1\cdot\boldsymbol{\tau}_2+1\rightleftharpoons 2\ , \end{aligned} \qquad (3.6)$$

where $g_{\rho\pi\gamma}$ and $G_{\rho\pi\gamma}(q)$ are the $\rho\pi\gamma$ coupling constant and form factor, respectively, and ϵ_{0123}=1. The value $g_{\rho\pi\gamma}$=0.56 is obtained from the measured width of the decay $\rho\rightarrow\pi\gamma$ [14], while the form factor is modeled, using vector-meson dominance, as

$$G_{\rho\pi\gamma}(q)=\frac{1}{1+q^2/m_\omega^2}\ , \qquad (3.7)$$

where m_ω is the ω-meson mass. Note that in Eq. (3.6) the term proportional to $k_1^\alpha k_1^\beta$ in the ρ-meson propagator has been dropped, since it vanishes if the nucleons are assumed to be on mass shell. Furthermore, in both meson propagators retardation effects have been neglected.

The leading terms in a non-relativistic expansion of Eq. (3.6) reduce to the familiar expressions for the $\rho\pi\gamma$ charge and current operators, as given, for example, in Ref. [2]. However, it is known that these lowest-order expansions, particularly that for $\mathbf{j}_{\rho\pi\gamma}$, are inaccurate. This fact was first demonstrated by Hummel and Tjon [15] in the context of relativistic boson-exchange-model calculations of the deuteron form factors, based on the Blankenbecler-Sugar reduction of the Bethe-Salpeter equation. It was later confirmed, in a calculation of the deuteron $B(q)$ structure function [2], that next-to-leading-order terms in the expansion for $\mathbf{j}_{\rho\pi\gamma}$, proportional $(1+\kappa_{\rho NN})/m^2$, very substantially reduce the contribution of the leading term. This issue will be returned to later in Sec. V. Here, again we stress that the full Lorentz structure of $j^\sigma_{\rho\pi\gamma}$ is retained in the present study.

IV. DEUTERON FORM FACTORS

The deuteron structure functions A and B, and tensor polarization T_{20} are expressed in terms of the charge (G_0 and G_2) and magnetic (G_1) form factors as

$$A(q) = G_0^2(q) + \frac{2}{3}\eta\, G_1^2(q) + \frac{8}{9}\eta^2 G_2^2(q) \ , \tag{4.1}$$

$$B(q) = \frac{4}{3}\eta(1+\eta)G_1^2(q) \ , \tag{4.2}$$

$$T_{20}(q) = -\sqrt{2}\frac{x(x+2)+y/2}{1+2(x^2+y)} \ , \tag{4.3}$$

where $\eta{=}(q/2m_d)^2$, $x{=}(2/3)\eta\, G_2(q)/G_0(q)$, $y{=}(2/3)\eta\,[1/2+(1+\eta)\,\mathrm{tg}^2\theta/2]\,[G_1(q)/G_0(q)]^2$, and θ is the electron scattering angle. The expressions above are in the Breit frame, and therefore q denotes the magnitude of the three-momentum transfer. The form factors are normalized as

$$G_0(0) = 1 \ , \quad G_1(0) = (m_d/m)\mu_d \ , \quad G_2(0) = m_d^2\, Q_d \ , \tag{4.4}$$

where μ_d and Q_d are the deuteron magnetic moment (in units of n.m.) and quadrupole moment, respectively, and are related to Breit-frame matrix elements of the nuclear electromagnetic charge, $\rho(\mathbf{q})$, and current, $\mathbf{j}(\mathbf{q})$, operators via:

$$G_0(q) = \frac{1}{3} \sum_{M=\pm 1,0} \langle \psi_M; \mathbf{v}_B \mid \rho(\mathbf{q}) \mid \psi_M; -\mathbf{v}_B \rangle \ , \tag{4.5}$$

$$G_1(q) = -\frac{1}{\sqrt{\eta}} \langle \psi_{M=1}; \mathbf{v}_B \mid j_{\lambda=1}(\mathbf{q}) \mid \psi_{M=0}; -\mathbf{v}_B \rangle \ , \tag{4.6}$$

$$G_2(q) = \frac{1}{2\eta} \left[\langle \psi_{M=0}; \mathbf{v}_B \mid \rho(\mathbf{q}) \mid \psi_{M=0}; -\mathbf{v}_B \rangle - \langle \psi_{M=1}; \mathbf{v}_B \mid \rho(\mathbf{q}) \mid \psi_{M=1}; -\mathbf{v}_B \rangle \right] \ . \tag{4.7}$$

Here $j_{\lambda=1}$ denotes the standard $+1$ spherical component of the current operator.

The calculations are carried out in momentum space. The wave functions $\psi_M(\mathbf{p}; \pm\mathbf{v}_B)$ are given in the second line of Eq. (2.7), and the charge and current operators are those described in Sec. III. The one-body current matrix elements involve the evaluation of integrals of the type, in a schematic notation,

$$\int \frac{\mathrm{d}\mathbf{p}}{(2\pi)^3} \psi_{M'}(\mathbf{p} + \mathbf{q}/4; \mathbf{v}_B)\, j^{\sigma}_{1-\mathrm{body}}(\mathbf{p}'_1, \mathbf{p}_1)\, \psi_M(\mathbf{p} - \mathbf{q}/4; -\mathbf{v}_B) \ , \tag{4.8}$$

with $\mathbf{p}'_1 = \mathbf{p} + \mathbf{q}/2$ and $\mathbf{p}_1 = \mathbf{p} - \mathbf{q}/2$, which are performed by standard Gaussian integrations. The two-body current matrix elements, instead, require integrations of the type

$$\int \frac{\mathrm{d}\mathbf{p}'}{(2\pi)^3} \frac{\mathrm{d}\mathbf{p}}{(2\pi)^3} \psi_{M'}(\mathbf{p}'; \mathbf{v}_B)\, j^{\sigma}_{2-\mathrm{body}}(\mathbf{k}_1, \mathbf{k}_2)\, \psi_M(\mathbf{p}; -\mathbf{v}_B) \ , \tag{4.9}$$

with $\mathbf{k}_1 = \mathbf{q}/2 + \mathbf{p}' - \mathbf{p}$ and $\mathbf{k}_2 = \mathbf{q}/2 - \mathbf{p}' + \mathbf{p}$. These integrations are efficiently done by Monte Carlo techniques by sampling configurations $(\mathbf{p}, \mathbf{p}')$ according to the Metropolis algorithm with a probability density $W(\mathbf{p}, \mathbf{p}') = w(\mathbf{p}) w(\mathbf{p}')$, where $w(\mathbf{p}) = p^2 \mid \psi_{M=0}(\mathbf{p}; 0) \mid^2$. The computer programs have been successfully tested by comparing, in a model calculation which ignored boost corrections and kept only the leading terms in the expansions for $j^{\sigma}_{1-\mathrm{body}}$ and $j^{\sigma}_{2-\mathrm{body}}$, the present results with those obtained with an earlier, configuration-space version of the code [2].

V. FURTHER RESULTS

In this section we briefly discuss the contribution of the $\rho\pi\gamma$ current to the $B(q)$ structure function. In Fig. 5 the results calculated with the current given in Eq. (3.6) (curve labelled $\rho\pi\gamma$-R) are compared with those obtained by using the leading term in its non-relativistic expansion (curve labelled $\rho\pi\gamma$-NR),

$$\mathbf{j}^{\rm NR}_{\rho\pi\gamma}(\mathbf{q}) = -\,{\rm i} g_{\rho\pi\gamma}\frac{g_{\rho NN}}{m_\rho}\frac{f_{\pi NN}}{m_\pi}G_{\rho\pi\gamma}(q)\frac{f_\rho(k_1)}{k_1^2+m_\rho^2}\frac{f_\pi(k_2)}{k_2^2+m_\pi^2}(\mathbf{k}_1\times\mathbf{k}_2)\,\boldsymbol{\sigma}_2\cdot\mathbf{k}_2\,\boldsymbol{\tau}_1\cdot\boldsymbol{\tau}_2 + 1\rightleftharpoons 2\ . \tag{5.1}$$

Figure 5 demonstrates the inadequacy of the approximation (5.1), a fact which, as mentioned already in Sec. III, has been known for some time [15]. Indeed a more careful analysis shows that the contributions of next-to-leading order terms are not obviously negligible, since they are proportional to the large ρNN tensor coupling constant, $\kappa_{\rho NN}$=6.1 in Ref. [13]. We sketch the derivation again here for the sake of completeness.

The vector structure $\epsilon_{i\nu\sigma\tau}\Gamma^\nu\,k_1^\sigma\,q^\tau$ occurring in Eq. (3.6), with $\Gamma^\nu=(\Gamma^0,\boldsymbol{\Gamma})$ defined as

$$\Gamma^\nu \equiv \overline{u}'_1\left(\gamma^\nu + {\rm i}\frac{\kappa_{\rho NN}}{2m}\sigma^{\nu\alpha}k_{1\,\alpha}\right)u_1\ , \tag{5.2}$$

can be written in the Breit frame as

$$\epsilon_{i\nu\sigma\tau}\Gamma^\nu\,k_1^\sigma\,q^\tau = \Gamma^0\ (\mathbf{q}\times\mathbf{k}_1) - k_1^0\ (\mathbf{q}\times\boldsymbol{\Gamma})\ , \tag{5.3}$$

where the index $i=1,2,3$ and $\mathbf{q}$=$\mathbf{k}_1+\mathbf{k}_2$. Up to order $(v/c)^2$ included, one finds, in analogy to the non-relativistic expansion of the nucleon electromagnetic current (with point-nucleon couplings, i.e. $F_1^S(q)\to 1$ and $F_2^S(q)\to\kappa_{\rho NN}$)

$$\Gamma^0 \simeq 1-(1+2\kappa_{\rho NN})\left[\frac{k_1^2}{8m^2}-\frac{\rm i}{4m^2}\boldsymbol{\sigma}_1\cdot(\mathbf{p}'_1\times\mathbf{p}_1)\right]\ , \tag{5.4}$$

$$\boldsymbol{\Gamma} \simeq \frac{1}{2m}(\mathbf{p}'_1+\mathbf{p}_1)+\frac{\rm i}{2m}(1+\kappa_{\rho NN})\,\boldsymbol{\sigma}_1\times\mathbf{k}_1\ . \tag{5.5}$$

Retaining only the leading term in Γ^ν, namely $\Gamma^\nu\simeq(1,0)$, leads to the expression in Eq. (5.1). Some of the corrections proportional to $\kappa_{\rho NN}$ were explicitly calculated in Ref. [2], and were found to decrease substantially those from the leading term.

We note, in passing, that the $\rho\pi\gamma$ charge operator, $\rho_{\rho\pi\gamma}(\mathbf{q})$, is proportional to

$$\epsilon_{i\nu\sigma\tau}\Gamma^{\nu}\, k_1^{\sigma}\, q^{\tau} = \mathbf{\Gamma}\cdot\mathbf{k}_1\times\mathbf{q}$$
$$\simeq \frac{\mathrm{i}}{2m}\,(1+\kappa_{\rho NN})\,\boldsymbol{\sigma}_1\cdot\mathbf{k}_1\times\mathbf{k}_2\ , \tag{5.6}$$

where the small non-local term proportional to $\mathbf{p}_1' + \mathbf{p}_1$ has been neglected. The standard form of the $\rho_{\rho\pi\gamma}(\mathbf{q})$ commonly used in studies of light nuclei form factors [10,11] easily follows. In this case too, however, higher order corrections included in $j^0_{\rho\pi\gamma}$, Eq. (3.6), reduce the contribution of the leading term, although they do not change its sign. A more detailed discussion of this issue will be given in Ref. [1].

We conclude this section with a couple of remarks. The first is that the destructive interference between the one-body and $\rho\pi\gamma$ currents is also obtained in recent calculations of the $B(q)$ structure function, carried out in the covariant framework based on the spectator equation [16,17].

The second remark is that in all earlier studies of light nuclei form factors [12] additional two-body currents, originating from the momentum-dependent terms of the two-nucleon potential, were included. Work is in progress [1] on an improved treatment of these currents, in an approach similar to that proposed in Ref. [18].

ACKNOWLEDGMENTS

The work of R.S. was supported by the U.S. Department of Energy contract DE-AC05-84ER40150, under which the Southeastern Universities Research Association (SURA) operates the Thomas Jefferson National Accelerator Facility. The work of V.R.P. was supported by the U.S. National Science Foundation via grant PHY 00-98353. Finally, most of the calculations were made possible by grants of computing time from the National Energy Research Supercomputer Center.

REFERENCES

[1] R. Schiavilla, to be published.

[2] R. Schiavilla and D.O. Riska, Phys. Rev. C **43**, 437 (1991).

[3] R.B. Wiringa, V.G.J. Stoks, and R. Schiavilla, Phys. Rev. C **51**, 38 (1995).

[4] U. van Kolck, Prog. Part. Nucl. Phys. **43**, 337 (1999).

[5] M. Walzl and U.-G. Meissner, Phys. Lett. **B513**, 37 (2001).

[6] J.L. Forest, V.R. Pandharipande, and A. Arriaga, Phys. Rev. C **60**, 014002 (1999).

[7] J.L. Forest, Phys. Rev. C **61**, 034007 (2000).

[8] J.L. Friar, Ann. Phys. (N.Y.) **104**, 380 (1977).

[9] G. Höhler, Nucl. Phys. B114, 505 (1976).

[10] L.E. Marcucci, D.O. Riska, and R. Schiavilla, Phys. Rev. C **58**, 3069 (1998).

[11] R.B. Wiringa and R. Schiavilla, Phys. Rev. Lett. **81**, 4317 (1998).

[12] J. Carlson and R. Schiavilla, Rev. Mod. Phys. **70**, 743 (1998).

[13] R. Machleidt, Phys. Rev. C **63**, 024001 (2001).

[14] D. Berg *et al.*, Phys. Rev. Lett. **44**, 706 (1980).

[15] E. Hummel and J.A. Tjon, Phys. Rev. Lett. **63**, 1788 (1989).

[16] J.W. Van Orden, N. Devine, and F. Gross, Phys. Rev. Lett. **75**, 4369 (1995).

[17] R. Gilman and F. Gross, `nucl-th/0111015`, J. Phys. G in press.

[18] K. Tsushima, D.O. Riska, and P.G. Blunden Nucl. Phys. **A 559**, 543 (1993).

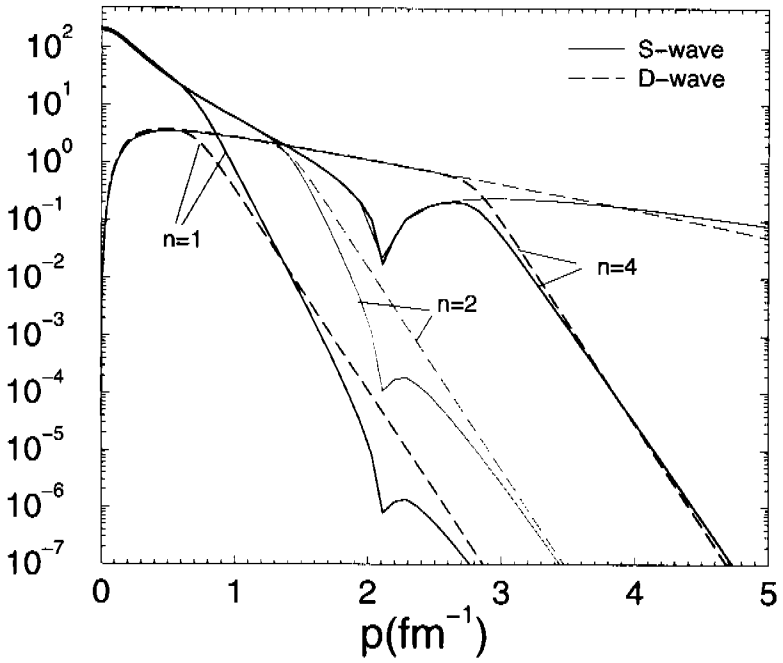

FIG. 1. The truncated wave functions $\overline{u}_L(p;n)$, with n=1, 2 and 4, are compared with the reference $u_L(p)$.

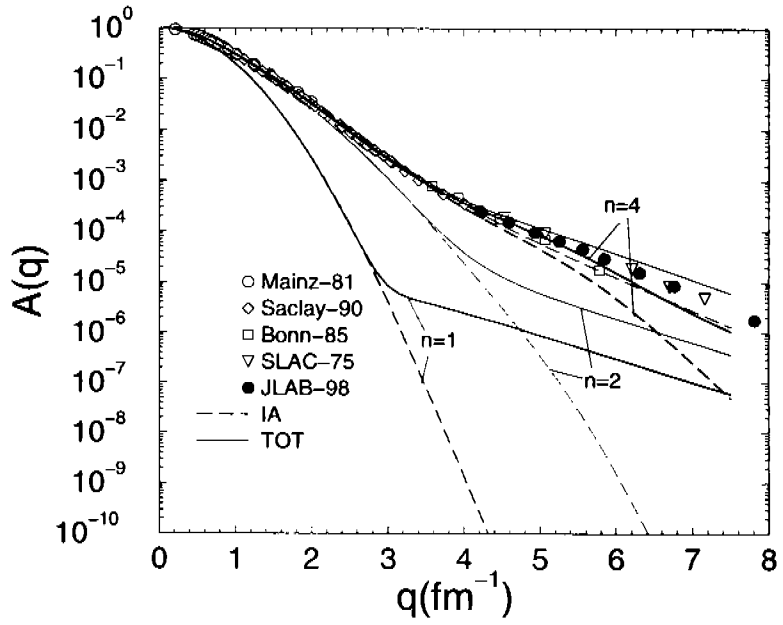

FIG. 2. The $A(q)$ structure functions obtained with the truncated wave functions $\overline{u}_L(p;n)$ for n=1,2, and 4 are compared with the reference $A(q)$ and data. The results obtained with one-body only and both two- and two-body operators, labelled respectively IA and TOT, are shown.

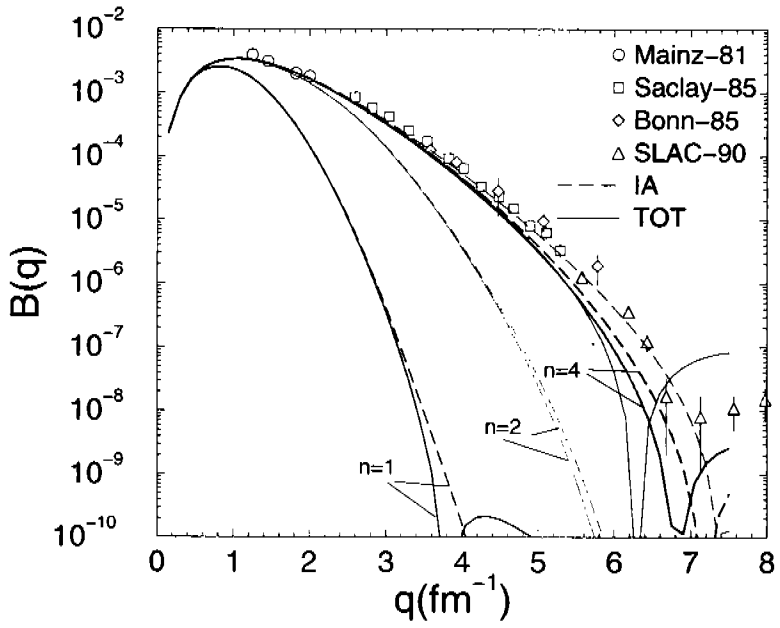

FIG. 3. Same as in Fig. 2, but for the $B(q)$ structure function.

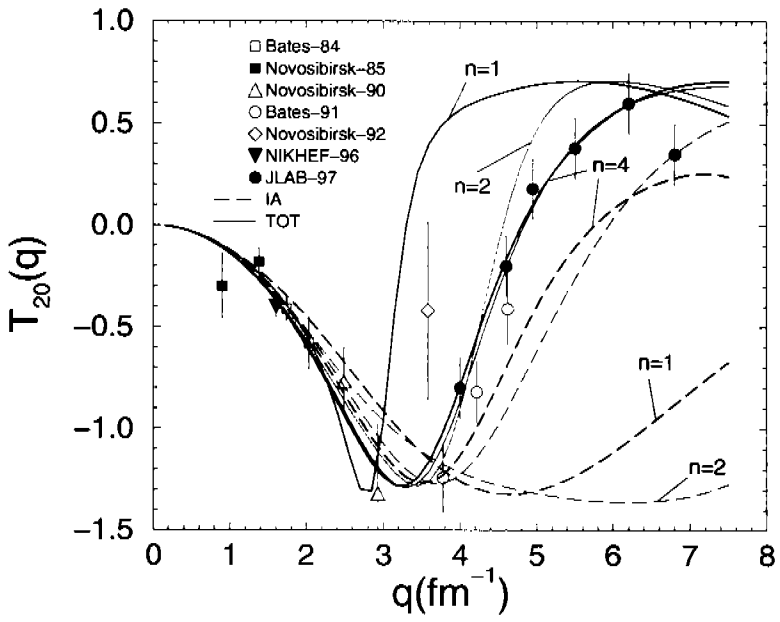

FIG. 4. Same as in Fig. 2, but for the $T_{20}(q)$ tensor polarization.

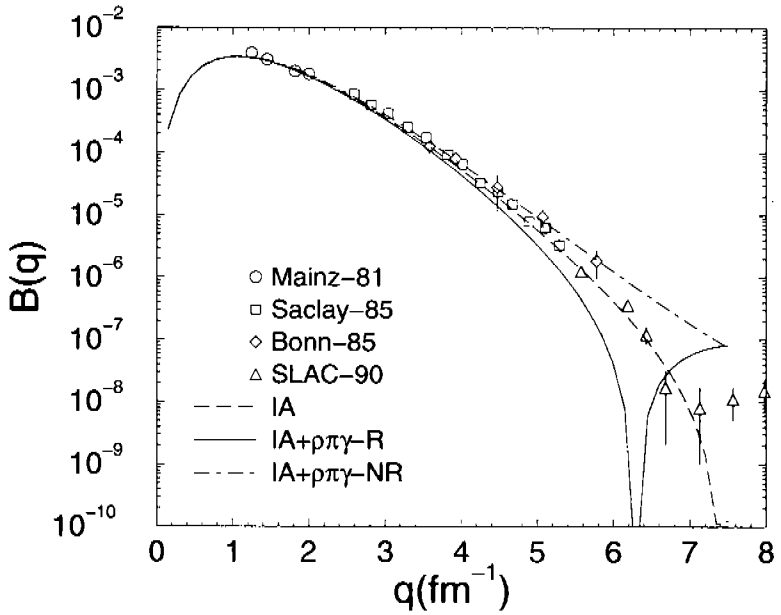

FIG. 5. The $B(q)$ structure functions obtained with the relativistic and non-relativistic forms of the $\rho\pi\gamma$ current of Eqs. (3.6) and (5.1), labelled respectively $\rho\pi\gamma$-R and $\rho\pi\gamma$-NR.